Advances in Science and Technology Research Journal

Advances in Science and Technology Research Journal, 2027, 21(1), 473–489
https://doi.org/10.12913/22998624/236056
ISSN 2299-8624, License CC-BY 4.0

Received: 2026.01.23
Accepted: 2026.11.15
Published: 2026.12.01

Structural reuse of recycled high-density polyethylene: Thermomechanical performance and service life of support arms for urban luminaires

Fredy Quicara Mamani[1], Iván Rafael Carpio Ayala[1], Jorge Luis Apaza Gutiérrez[1], Waygand Freddy Beltrán Quispe[1*]

[1] Universidad Nacional de San Agustín de Arequipa, Arequipa 04000, Perú
* Corresponding author email: wbeltranq@unsa.edu.pe

ABSTRACT

The accumulation of post-consumer plastic waste poses a critical challenge to sustainable urban infrastructure. This study evaluates the nonlinear thermomechanical behavior and lifespan of a street light support made from recycled high-density polyethylene reinforced with 30% glass fiber (r-HDPE/GF30%). Using a multiphysics computational framework that integrates finite element analysis (ANSYS) with large deflections and temperature-dependent plasticity, three geometric configurations are compared: circular (G1), rectangular (G2), and variable elliptical (G3) cross-sections. Under severe loading conditions at 100 °C, the results demonstrate that the conventional geometries (G1 and G2) exhibit structural instabilities and a state of severe instability, with Safety Factors (SF) of 0.26 and 0.29, respectively. In contrast, the optimized G3 configuration mitigates thermal softening through efficient redistribution of internal stresses, achieving a factor of safety (FS) of 1.57 and a controlled maximum deformation of 149 mm. A sigmoidal decay kinetic model, calibrated with the numerical results, projects a service life of 10.4 years for the G3 profile compared to 5.8 years for the rectangular design, representing a 79% service extension. These findings validate that geometric optimization is a strategic requirement for the viable implementation of recycled composite materials in long-life portable infrastructure, promoting the transition to urban circular economy models.

Keywords: recycled high-density polyethylene, glass fiber (GF30%), finite element analysis, large deflections, urban infrastructure, viscoelastic creep.

INTRODUCTION

The exponential accumulation of post-consumer plastic waste represents one of the most critical environmental and logistical challenges for sustainable urban development globally. In this context, the transition from conventional recycling schemes to upcycling models is positioned as a fundamental strategy for reinserting polymeric materials into high value-added life cycles [1–3]. Within the infrastructure of smart cities, street furniture and lighting are essential elements that demand a comprehensive design focused not only on energy efficiency and sustainability, but also on mechanical durability under outdoor service conditions [4]. Despite its abundance in waste streams, the reuse of unreinforced recycled high-density polyethylene (r-HDPE) in structural support applications faces serious operational limitations. r-HDPE suffers severe thermal softening, high susceptibility to creep dependent on temperature and applied stress, as well as progressive degradation caused by ultraviolet radiation [5, 7]. Furthermore, prolonged exposure to solar radiation and extreme heating cycles triggers thermo-oxidative degradation processes in the polymer matrix, altering its rheological behavior and drastically reducing its initial elastic modulus [8–10]. To overcome these inherent deficiencies

of the pure thermoplastic matrix, the incorporation of 30% by weight fraction of short glass fibers (r-HDPE/GF30%) allows for the creation of a composite material with superior mechanical stiffness, increased tensile strength, and remarkable dimensional stability under thermal gradients [11–13].

From a numerical modeling perspective, predicting the thermomechanical response of elements made with randomly oriented fiber-reinforced composites requires advanced computational frameworks capable of reproducing stress transfer at the matrix-fiber interface [14, 15]. When slender geometric components made of r-HDPE/GF30% are subjected simultaneously to thermal peaks from solar radiation (which can reach up to 100 °C) and permanent gravitational loads, the classical assumption of static linear elasticity proves mathematically insufficient [16]. The loss of stiffness coupled with the softening of the amorphous phase of the polymer induces states of plastic deformation and geometric instabilities. Therefore, finite element analysis (FEA) must necessarily integrate temperature-dependent plasticity formulations and large deflection geometric nonlinearity effects to accurately capture flexural-torsional buckling phenomena and avoid divergent or unrealistic numerical solutions [17, 18]. Despite the existing body of literature on the behavior of reinforced thermoplastics, a knowledge gap persists regarding how the transverse geometric optimization of support elements can mitigate the loss of thermomechanical stiffness in r-HDPE/GF30% components exposed to extreme solar radiation peaks.

The main objective of this study is to numerically evaluate the nonlinear thermomechanical performance and structural stability of a support arm for urban luminaires made from a 30% glass fiber reinforced r-HDPE composite (r-HDPE/GF30%). Using a multiphysics framework in ANSYS that considers temperature-dependent plasticity (BISO model) and geometric nonlinearity due to large deflections, three geometric configurations are compared: the conventional circular section (G1), the rectangular section (G2), and a proposed elliptical section with variable geometry (G3). This work demonstrates how the geometric redistribution of inertia in the optimized elliptical section (G3) effectively counteracts the thermal softening of the polymer at 100 °C, guaranteeing mathematical convergence, reducing structural deflection to safe service limits and consolidating the upcycling of reinforced plastics in urban infrastructure.

CASE STUDY AND DESIGN CONFIGURATIONS

This section defines the physical problem by describing the luminaire support, its function, its service conditions, and the geometric alternatives. The objective is to establish a realistic framework where the thermomechanical responses are directly related to the optimization of the cross-sectional geometry and the nonlinear behavior of the composite material.

Support for urban luminaires – geometry and service conditions

The component analyzed is a support arm for urban public lighting, composed of an upward-curved segment and two straight tubular segments connected by a structural elbow. This configuration results in a vertical height of 2.565 m, while the effective structural length, which governs the maximum bending moments, is 4.571 m [4]. From a structural perspective, the support functions as a slender cantilever beam, which is inherently susceptible to instability and large geometric deflections [18]. The highest levels of Von Mises stress and deformation are expected to be concentrated in the connection or embedment zone to the main pole. This stress state is driven by permanent mechanical loads, corresponding to the combined action of the self-weight of the r-HDPE/GF30% arm and the mass of the luminaire installed at the free end.

Environmentally, the support is subject to continuous exposure to the elements, where solar radiation constitutes the dominant thermal load. Given the thermal conductivity of the r-HDPE/GF30% composite and the wall thickness of the profile, the structure is prone to reaching a saturated thermal steady state during peak sunlight hours. To assess structural viability under the worst-case scenario, a uniform peak operating temperature of 100 °C is established. This critical thermal load, acting simultaneously with gravitational loads, induces a drastic softening in the amorphous phase of the polymer matrix, which accelerates the loss of stiffness and makes the use of elastoplastic models indispensable to predict the collapse or stabilization of the part.

Functional requirements and service conditions

To evaluate the influence of shape on thermomechanical behavior, three configurations were modeled (Figure 1). All designs share the same overall height, effective structural length, and luminaire dimensions (Figure 2) to ensure functional consistency according to urban lighting requirements (Table 1). This configuration allows for an objective comparison to determine the stiffness-to-weight ratio and thermal resistance of the structure.

Circular section (G1): Conventional design with a constant wall thickness of 10 mm, serving as the structural base.

Rectangular section (G2): A simplified manufacturing alternative with a constant wall thickness of 10 mm. Its sharp corners are expected to contribute to stress concentrations.

Variable elliptical section (G3): Design with a functional gradient where the wall thickness decreases from 10 mm at the base to 6 mm at the free end. This geometry is designed to improve material distribution and reduce aerodynamic drag.

Material characterization and cross-sectional alternatives

Recycled high-density polyethylene (r-HDPE) offers significant availability and high reuse potential [1, 2]. However, its inherently low stiffness and high susceptibility to thermal softening limit its standalone application in load-bearing urban infrastructure [3]. To overcome these thermomechanical barriers, a short glass fiber

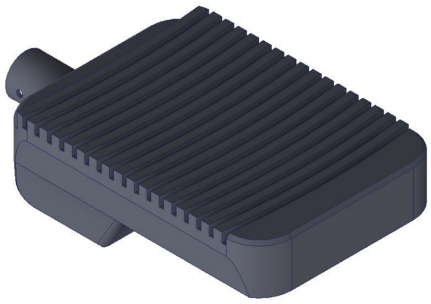


Figure 2. Standardized geometric configuration of the luminaire used for thermostructural simulation in all support profiles (G1, G2 and G3)

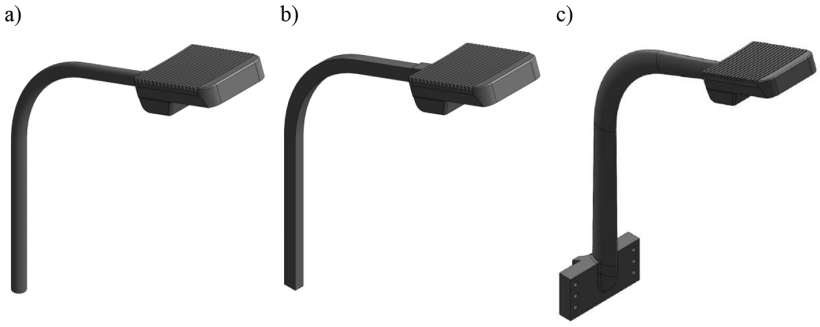


Figure 1. Geometric configurations of the luminaire support: a) constant circular cross-section, b) constant rectangular cross-section and c) variable elliptical cross-section

Table 1. Geometric parameters and mass properties of the luminaire support configurations

Parameter	G1 (circular)	G2 (rectangular)	G3 (variable elliptical)
Cross-section type	Constant	Constant	Tapered
Wall thickness (mm)	6.0	6.0	10.0 → 6.0
Base dimensions (mm)	Ø110	98 $\times$ 68	260 × 140
Top dimensions (mm)	Ø110	98 $\times$ 68	170 × 95.03
Cross-sectional area (mm^2)	1.960	1.848	5.969
Moment of inertia *I* (mm^4)	2.66×10^6	2.37×10^6	39.35×10^6
Section modulus *S* (mm^3)	4.84×10^4	4.83×10^4	3.02×10^5
Volume (m^3)	0.0065	0.0071	0.0066
Mass (kg)	7.605	8.307	7.722

Note: The area, moment of inertia, and section modulus are calculated at the fixed base connection, where the bending moment is maximum. Bending is considered along the main vertical load axis. The mass was calculated assuming a material density of $\rho = 1170$ kg/m³.

reinforced composite (r-HDPE/GF) was selected. This material, unlike pure r-HDPE, has improved mechanical properties, as demonstrated in the polymer engineering literature [11, 13].

The specific thermomechanical characteristics of this composite—including its density, coefficient of thermal expansion, and temperature-dependent mechanical limits—are detailed in Table 2, using structural steel as a reference. Experimental characterizations of HDPE hybrid composites indicate that incorporating approximately 30–40% treated glass fibers can raise the tensile modulus to values exceeding 5 GPa [11, 12]. However, recognizing the inherent heterogeneity present in post-consumer recycled raw materials, a conservative engineering approach was adopted for the numerical model. The literature reports that HDPE composites reinforced with 30% high-quality glass fiber can achieve a tensile modulus exceeding 5.0 GPa. However, acknowledging the intrinsic heterogeneity and potential interfacial variability in post-consumer recycled raw materials, the maximum theoretical modulus was intentionally penalized. For this study, a reference modulus of elasticity of 4140 GPa and a yield strength of 48 MPa were established for the simulated r-HDPE/GF composite. This methodological reduction assumes the worst-case scenario, ensuring that the structural design is safe and viable even if the recycled material does not maintain optimal properties, as mentioned in the literature [3, 11].

Critically, instead of assuming simple linear degradation that can induce non-physical singularities at maximum temperatures, the study incorporates temperature-dependent stiffness and yield strength defined using discrete tabular data [14–16]. This modeling approach, which accurately captures localized softening and the resulting mechanical gradients along the structure, is based on previous experimental findings demonstrating a consistent correlation between thermal exposure and stiffness reduction in recycled polymers [5–9]. This relationship is a critical factor for structural components subjected to direct solar radiation, where temperature variations between the surface and the core determine overall stability [4, 10].

NUMERICAL AND MULTIPHYSICS MODELING

This section describes the numerical framework adopted to evaluate the thermomechanical response and long-term durability of urban luminaire supports. The strategy employs a hybrid computational approach: Finite Element Analysis (FEA) using ANSYS to determine spatial thermal and stress fields, and Stochastic Kinetic Modeling using Python to extrapolate material integrity. This two-layered methodology ensures that both localized structural gradients and temporal

Table 2. Thermomechanical properties of reduced glass fiber reinforced high density polyethylene (r-HDPE/GF) and structural steel

Property	Symbol	r-HDPE / GF (reinforced)	Structural steel	Units
Density	ρ	1170	7850	kg/m³
Young's modulus (25 °C)	$E_{25°}$	4.140	200	GPa
Poisson's ratio	v	0.35	0.30	–
Yield strength (25 °C)	$\sigma_y 25°$	48	250	MPa
Thermal conductivity	k	0.42	45	W/m·K
Specific heat	C_p	1150	470	J/kg·K
Coefficient of thermal expansion	α	40×10^{-6}	12×10^{-6}	1/°C
Yield strength at 60 °C	$\sigma_y 60°$	48	247	MPa
Young's modulus (60 °C)	$E_{60°}$	2.5	200	GPa
Yield strength at 90 °C	$\sigma_y 90°$	18	245	MPa
Young's modulus (90 °C)	$E_{90°}$	0.85	200	GPa

Note: For the r-HDPE/GF composite, structural degradation was modeled using discrete, temperature-dependent tabular data, ranging from 20 °C to 90 °C, to accurately reflect the material's thermoelastic transition and avoid non-physical singularities at the point of maximum solar exposure. The steel properties were assumed to remain virtually unchanged within the analyzed temperature range.

degradation kinetics are captured following established coupling procedures for large-scale thermomechanical simulations [16].

Thermal model under solar radiation

The thermal response was evaluated under steady-state conditions, simulating prolonged exposure to a maximum solar irradiance (G) of 1000 W/m² [10]. Considering that the material is not a completely black body and has an absorptivity of 0.65, at which point the structure would absorb 650 W/m², this approach is used because simulating it as a black body would absorb the full 1000 W/m², causing the material to approach its melting point, at which point it would enter a highly viscous state. This environmental boundary condition is modeled as a multimodal heat transfer problem, where solid-state conduction and surface-to-environment exchange are coupled to reflect the real-world solar gain.

Conductive heat transfer within the r-HDPE/GF solid is governed by Fourier's law, expressed in Equation 1, where the thermal conductivity parameters were obtained from experimentally validated literature [9, 12].

$$k\nabla^2 T = 0 \tag{1}$$

where: k represents the isotropic thermal conductivity of r-HDPE/GF (0.45 W/m·K).

Following fundamental thermodynamic principles for environmental exposure, the internal temperature distribution is assumed to be driven by the balance between solar absorption and atmospheric cooling. To maintain computational efficiency without sacrificing physical relevance, surface heat exchange is driven by a nonlinear energy balance. This boundary condition is essential for polymers, as their low thermal conductivity often leads to high surface temperatures. The net heat flux (q_{net}) at the boundaries is defined by Equation 2, which integrates solar absorption, natural convection, and radiative emission:

$$-k\frac{\partial T}{\partial n} = \alpha G - \\ -[h_c(T_S - T_\infty) + \epsilon\sigma(T_S^4 - T_{surr}^4)] \tag{2}$$

To simulate the worst-case scenario corresponding to a critical hot day with low wind speed, a conservative natural convection coefficient of h_c = 10 W/m²·K was assigned to the external surfaces exposed to the open air. A thermal emissivity of ε = 0.85, typical for HDPE, was also assumed. The ambient and radiative environment temperatures (T_∞, T_{surr}) were set at 35 °C as the ambient baseline. These boundary conditions ensure that the simulated peak temperatures accurately reflect stagnation heating under maximum solar irradiance.

In this formulation, α is the solar absorptivity, h_c is the convection coefficient, and εσ represents the radiation parameters. This approach, widely validated in the literature for outdoor thermal performance [4, 10], isolates the maximum temperature levels and spatial gradients that govern subsequent material degradation analysis.

Mechanical load and boundary conditions

Structural integrity was evaluated under a conservative multiaxial load combination designed to simulate extreme urban operating conditions. The mechanical equilibrium of the cantilever system is governed by the sum of forces and moments, which supports the internal stress distribution reflecting the effects of gravity. Table 3 summarizes the structural loading scenarios and gravity specifications applied to the finite element model. These parameters were kept identical for all design identifiers (G1, G2, G3) to ensure that variations in performance are strictly attributable to the cross-sectional geometry and its corresponding moment of inertia. The total mechanical moment (M_{total}) at any section x along the arm is expressed in Equation 3:

$$M_{total}(x) = \sum M_{gravity} \tag{3}$$

The total mechanical moment at any section x along the arm is derived exclusively from gravitational loads (self-weight and weight of the luminaire assembly), omitting aerodynamic pressures to isolate the effect of thermo-mechanical degradation.

As stated in Equation 4, and in accordance with the moment-area theorem discussed by Hibbeler, the structural displacement (δ) is a function of the integral of the curvature weighted by the lever arm ($L - x$) relative to the free end and the variable moment of inertia (I_x), which is the main differentiator in this study. The 99.68% reduction in strain observed in the strain response under the coupled load section is a direct consequence of

Table 3. Structural loading scenarios: Gravity forces and specifications

Load case	Symbol	Magnitude	Units	Application	Description
Gravitational acceleration	g	9.8066	m/s²	Global	Standard Earth gravity
Self-weight	–	Calculated	–	Volume	Derived from material density
Luminaire weight	F_1	49.05	N	Free end	Equivalent to 5 kg mass
Secondary operational load	F_2	68.67	N	Arm region	Conservative additional load
Support condition	–	Fixed	–	Base	Fully constrained

the strategic variation of this geometric parameter under the loads defined in Table 3, which effectively increases the flexural stiffness (EI) where the bending moment is maximum.

$$\delta = \int_0^L \frac{M(x)}{E(T)I(x)}(L-x)dx \tag{4}$$

In the computational environment, these loads were applied as vectorized boundary conditions to ensure directional accuracy. As illustrated in Figure 3, the gravitational components, comprising the luminaire assembly (F_1) and the secondary operating load (F_2), were modeled as remote forces localized at the free end of the arm. The global gravitational vector was enabled to account for the structure's self-weight, while the base was defined as a fixed support, restricting all nodal translations and rotations.

Thermomechanical coupling and degradation kinetics

A one-way sequential coupling scheme was implemented using the nodal temperature field as the primary coupling variable. The steady-state thermal solution is applied to the structural mesh as a volumetric load, inducing internal stresses through differential expansion. This strategy is physically justified by the assumption that thermal effects govern the mechanical behavior of the r-HDPE/GF composite, while structural deformations are insufficient to significantly alter the temperature distribution.

Critically, the local temperature governs the variation of the material's stiffness and yield strength. To avoid non-physical singularities associated with linear extrapolation models, the temperature-dependent material behavior is defined using discrete tabular data points (Table 2). The finite element solver uses piecewise linear interpolation between these experimental data points to continuously map stiffness degradation and yield surface reduction. This approach is consistent with reported stiffness-temperature correlations for reinforced polymers, providing a validated basis for subsequent structural simulations.

Within the evaluated range (20–90 °C), the composite remains strictly in its solid phase, well below its melting point, justifying a thermoelastic constitutive approach.

To link these static FEA results with long-term durability, a cumulative damage model was integrated using Python. The degradation rate (K) follows the Arrhenius Law, which correlates maximum nodal temperatures (T_{max}) with the rate of chemical bond rupture in the polymer chain. As detailed in the established experimental literature on the thermo-oxidative aging of polymers [8, 9], this is expressed in Equation 5:

$$K(T) = A.\exp\left(-\frac{E_a}{R.T_{peak}}\right) \tag{5}$$

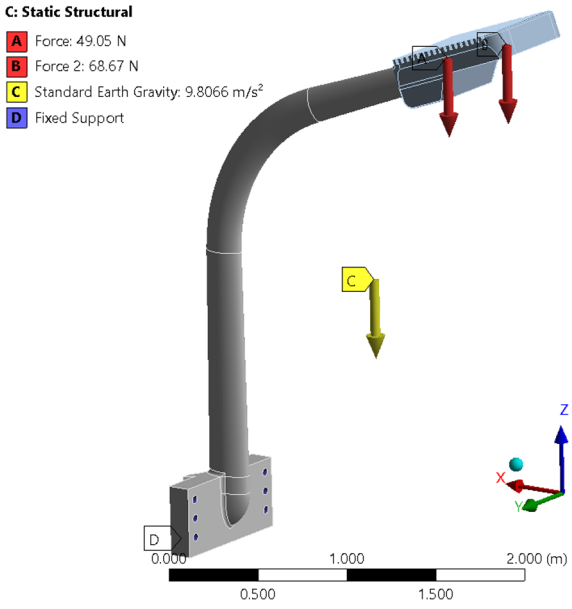


Figure 3. Boundary conditions and multidirectional loading configuration for thermomechanical analysis

Table 4. Parameters used in the Arrhenius equation based on experimental literature

Parámeter	Symbol	Value
Pre-exponential factor	A	0.001 h^{-1}
Energy activation	E_a	0.05 eV

This kinetic rate is then used to solve for the sigmoidal integrity decay function, allowing the localized thermal and stress data to be transformed into the lifetime projections (10.4 years for G3) presented in the results section. This coupling supports a mathematically coherent transition from a 7-day environmental cycle to a ten-year lifetime, grounded in polymer thermodynamics (Table 4).

Discretization and convergence criteria

Numerical discretization was performed using 20-node three-dimensional quadratic solid elements (SOLID186) to accurately capture the coupled thermomechanical stress gradients within the structure [16]. Mesh independence was assessed through a systematic refinement study by monitoring the stabilization of the maximum total strain (δ_{max}), selected as the primary convergence indicator [17, 18]. Following verification protocols for nonlinear finite element analysis, the relative variation (Δ) between successive mesh densities was evaluated according to Equation 6:

$$\Delta(\%) = \frac{|\delta_i - \delta_{i-1}|}{\delta_{i-1}} \times 100 \qquad (6)$$

The results of the refinement process, summarized in Table 5, demonstrate the model's response under the geometrically nonlinear formulation (Large Deflection = ON). While the reference geometries G1 and G2 exhibit numerical instability and a lack of convergence due to physical collapse and elastic instability induced by thermal softening (100 °C), the optimized geometry G3 achieved progressive stabilization of the total deformation and Von Mises stresses. For the final mesh configuration adopted in profile G3, the relative variation (δ) between successive refinements remained strictly below the 5% threshold, confirming that the numerical results for the proposed structure are independent of the discretization scale.

Figure 4 illustrates the convergence behavior of the normalized mesh of the three geometric configurations, based on the stabilization of the maximum total strain. Despite significant differences in absolute strain levels among the variable circular, rectangular, and elliptical profiles,

Table 5. Mesh convergence index and summary of numerical stability

Design ID	Element (n)	Deformatión (mm)	Von mises (MPa)	Relative var (%)	Estate
G1 – circular	57412	3487.20	53.62	–	–
	48437	4112.60	56.75	5.84	Not converge
	42553	3771.40	39.53	30.34	Not converge
	39185	3700.40	41.84	5.84	Not converge
	39116	3282.60	36.98	11.62	Not converge
	37909	3462.00	40.22	8.76	Not converge
G2 – rectangular	67668	1211.50	38.01	–	–
	46502	1210.50	37.86	0.39	Converge
	36666	1209.40	38.1	0.63	Converge
	33434	1208.30	38.45	0.92	Converge
	31948	1206.80	37.44	2.63	Converge
	30812	1205.70	38.81	3.66	Converge
G3 – variable eliptical	70519	149.0	5.08	–	–
	62864	149.04	5.06	0.39	Converge
	59554	149.02	5.06	0.00	Converge
	58037	149.03	5.07	0.20	Converge
	56487	149.01	5.04	0.59	Converge
	54802	149.02	5.06	0.40	Converge

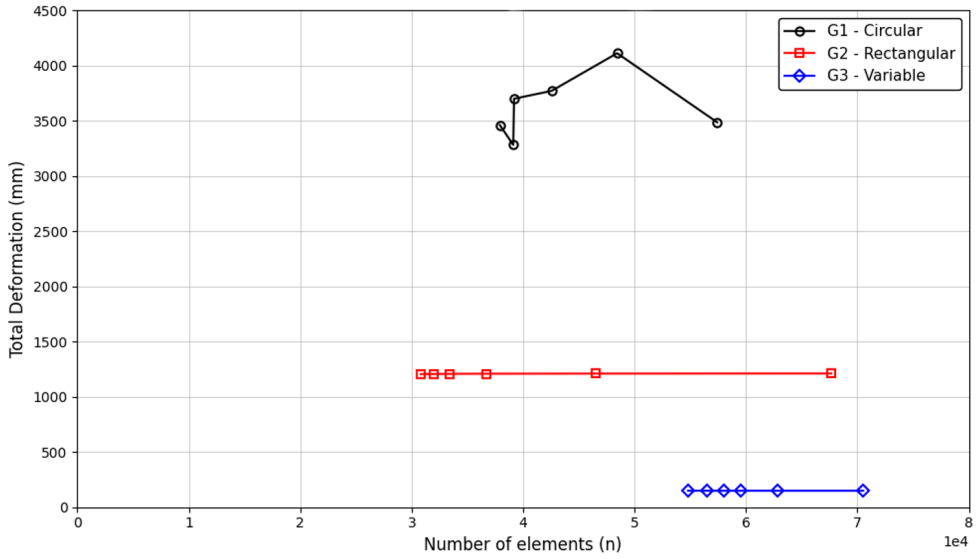


Figure 4. Normalized mesh convergence of the maximum total deformation for the three geometric configurations

all designs show a clear asymptotic trend as the number of elements increases.

It is worth noting that the variable elliptic configuration (G3) achieves convergence with minimal relative strain increase, accompanied by stabilization of the equivalent Von Mises stresses. This indicates low sensitivity to mesh refinement, attributable to a more uniform distribution of stresses and thermal gradients. This behavior not only supports the numerical robustness of the optimized geometry but also confirms that the adopted mesh densities guarantee solution independence, thus optimizing computational cost.

Model assumptions and limitations

To maintain computational rigor in the comparative geometric analysis and address the complex nature of the material under coupled loads, the numerical model was based on the following thermomechanical considerations:

- Macroscopic behavior and inelasticity: The r-HDPE/GF composite was modeled as a continuous and quasi-isotropic medium at the macroscopic level. This mathematical approximation is justified by the three-dimensional distribution and random orientation of the short fibers after the extrusion process. To overcome the limitations of a purely linear elastic model, a temperature-dependent Bilinear Isotropic Hardening (BISO) elastoplastic model was implemented, capturing the thermal softening of the matrix and the yield strength where permanent deformation occurs. Furthermore, geometric nonlinearity effects (Large Deflection) were incorporated to accurately record any structural instability or buckling.
- Conservative creep criterion: No explicit tracking of the long-term plastic creep curve or post-failure tearing was performed. Instead, the research adopted a preventive design strategy based on the Serviceability Limit State (SLS). The analysis focused on identifying the geometric instability threshold under thermal peaks, ensuring that, through geometry optimization, sustained stresses are drastically reduced, remaining in a regime where long-term viscous deformations do not compromise structural function.
- Environmental degradation factors: While the service life model rigorously considers thermal matrix degradation and viscoelastic decay, it does not currently incorporate the synergistic effects of UV photodegradation or moisture absorption. These exclusions, along with the assumption of ideal load transfer (perfect adhesion) at the fiber-matrix interface, set up a conservative baseline scenario designed to isolate and strictly evaluate the thermomechanical feasibility of the geometric configurations.

RESULTS AND DISCUSSION

This section presents the numerical results obtained from the coupled thermomechanical analysis of the r-HDPE/GF urban luminaire

support. The results are organized to describe the thermal response, the resulting degradation indicators, and the associated structural behavior under combined loading conditions. All simulations were performed under identical environmental and mechanical conditions to ensure a rigorous geometric comparison.

Steady-state temperature fields and thermal gradients

The thermal analysis performed in ANSYS Steady-State Thermal reveals that solar radiation induces non-uniform temperature fields, characterized by high surface localization due to the low thermal conductivity of the r-HDPE/GF composite (reference). As shown in Figure 5, under the maximum heat flux, considering the worst-case scenario of a hot day with temperatures reaching 35 °C (the reference point for the simulations), surface heating varies depending on the geometric area exposed to radiation: the variable elliptical design (G3) reaches a peak of 100 °C, the rectangular section (G2) registers approximately 97 °C, and the circular profile (G1) exhibits the lowest surface value at 93 °C (see Figure 6 for the detailed distribution).

Although G3 registers the absolute maximum temperature due to its larger direct exposure area, maximizing geometric inertia, the critical advantage of this design lies not in avoiding heat absorption, but in its exceptional management of the thermal gradient along the structure. Despite operating under the most severe thermal regime (100 °C), G3 exhibits a much more gradual and fluid longitudinal heat distribution. In stark contrast, although G2 and G1 experience slightly lower thermal peaks, their topologies are mechanically inefficient in the face of plastic softening: G2 detrimentally concentrates thermal stress at the orthogonal corners of its base, while G1 suffers critical differential softening that induces instability. The optimized topology of G3 effectively mitigates these thermo-mechanical stress concentrations, ensuring stability even in its most critical thermal state.

Thermal gradients and degradation indicators

The long-term structural viability of the support is intrinsically governed by the thermomechanical degradation kinetics and creep behavior of the polymer composite under prolonged thermal exposure. Figure 7 quantifies the coupled influence of material thermal decay and geometric inertia on system integrity. As detailed in Figure 7a, under sustained exposure to 60 °C, the elliptical profile material (G3) exhibits pronounced nonlinear viscoelastic relaxation. The

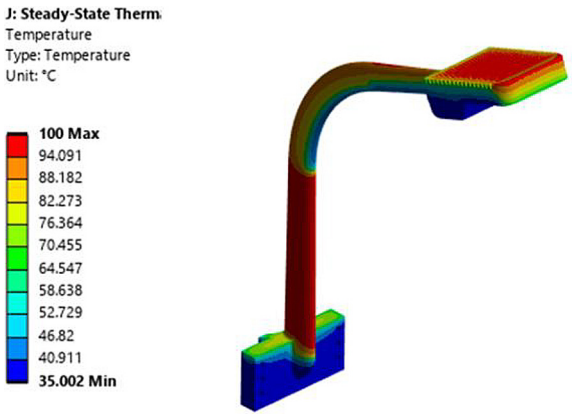


Figure 6. Distribution of imported body temperature on the variable elliptical r-HDPE/GF lighting support

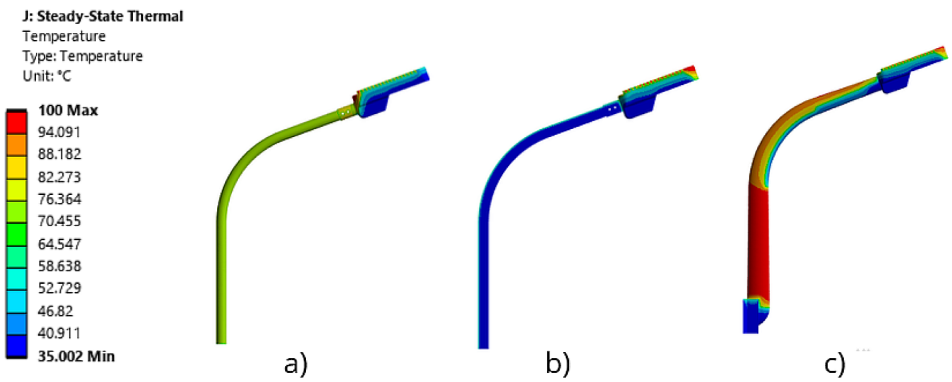


Figure 5. Distribution of imported body temperature under solar radiation: a) circular section (G1), b) rectangular section (G2) and c) variable elliptical section (G3)

composite loses approximately 80% of its initial stiffness within the first 500 hours of exposure, at which point the decline stabilizes upon reaching the residual elastic modulus provided by the glass fiber network. While this drastic reduction underscores the inherent risks of using recycled plastics in high-thermal-demand environments, the comparative analysis (Figure 7b) reveals the true impact of geometric optimization. Faced with this same critical threshold of material degradation, the G3 topology compensates for the loss of intrinsic stiffness through superior stress management, maintaining a safe stability profile over extended timescales. In stark contrast, the inefficient load distribution in the rectangular section (G2) and the circular profile (G1) precipitates irreversible geometric instabilities and large deflections, leading them to states of severe instability significantly prematurely.

While the degradation curves in Figures 7 and 8 assume constant isothermal exposure, they provide a conservative analytical framework for the worst-case design scenario. In real urban environments, the cumulative nature of thermo-oxidative aging means that the peak thermal loads identified during the day act as the primary driver of long-term polymer embrittlement, overcoming the recovery effect of nighttime cooling cycles.

Complementing the stiffness loss analysis, Figure 8 characterizes the "High Failure Zone" using the ductility retention kinetics of the r-HDPE/GF composite under exposure to thermal gradients of 25, 60, 90, and 100 °C. As evidenced by the curve trend at 90 °C, the rectangular profile (G2), which experiences localized critical temperatures up to a maximum of 100 °C, undergoes "Rapid Ductility Loss." Under these severe thermal conditions, the normalized elongation at break of the material collapses precipitously below the critical brittleness threshold (50%) in approximately 70 hours. Furthermore, the 100 °C curve illustrates the extreme limit of this behavior, revealing an almost immediate structural collapse.

This accelerated thermal embrittlement is driven jointly by the steep temperature gradients through the thickness and the progressive degradation of the bond at the fiber-matrix interface. This microstructural deterioration drastically reduces the component's toughness and its ability to dissipate kinetic energy from cyclic dynamic loads, such as wind-induced aerodynamic vibrations. Consequently, this mechanical exhaustion marks the definitive transition from a stable elastic performance regime to premature and severe structural failure of the infrastructure.

Deformation response under coupled loading

The mechanical integrity of the r-HDPE/GF composite support was evaluated by correlating localized thermal softening with multidirectional loading. The results demonstrate that the structural behavior is strictly determined by the efficiency of the cross-section in redistributing internal stresses under thermal gradients induced by solar radiation.

The total deformation results reveal a critical disparity in behavior between the reference profiles (G1 and G2) and the proposed variable elliptical geometry (G3). As detailed in Table 6, the circular profile (G1) develops a maximum theoretical displacement of 3487.2 mm (3.487 m). This extreme value, which exceeds the total length of the structural model, is interpreted as a state of severe structural failure due to flexural-torsional

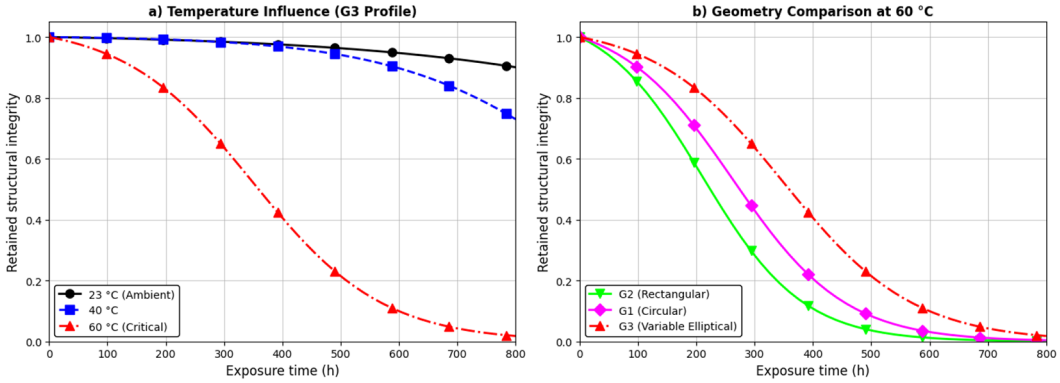


Figure 7. Thermomechanical integrity of r-HDPE: a) influence of exposure temperature and b) comparative geometric retention at 60 °C

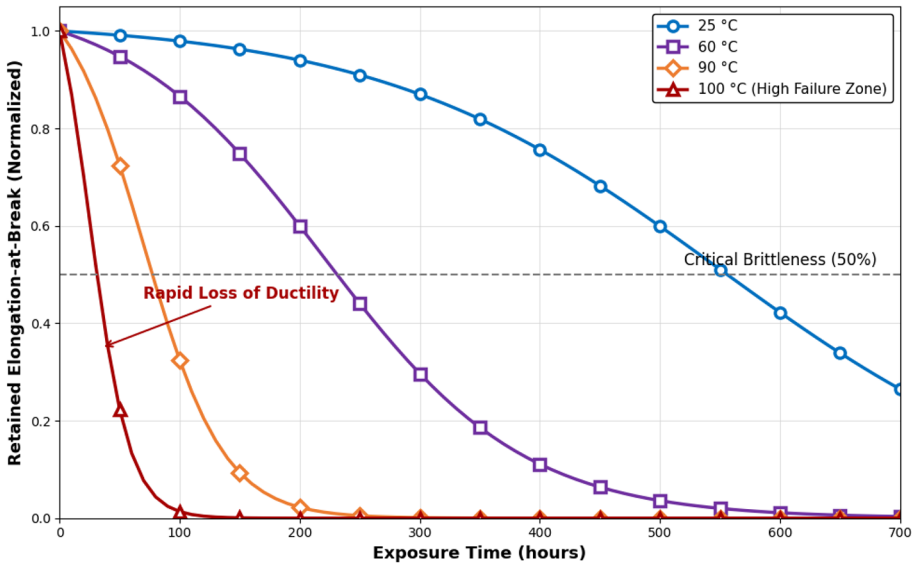


Figure 8. Thermal aging of the r-HDPE/GF composite: Ductility retention kinetics and failure thresholds under critical exposure

collapse rather than stable equilibrium. This disproportionate behavior is explained by the material softening formulation, supported by the kinetics of Equation 5 and the discrete thermoelastic data defined in Table 2. As the local temperature reaches its maximum values, the modulus of elasticity E(T) and the yield strength $\sigma_y(T)$ of the polymer matrix decrease significantly. Because the conventional profile G1 has a constant and low moment of inertia I(x), it cannot compensate for this severe thermally induced stiffness loss. This indicates that a circular cross-section lacks the necessary inertia to counteract the thermal softening of the r-HDPE/GF composite, degrading the elastic modulus to a point where the structure experiences high deflection instability.

Similarly, the rectangular profile (G2) showed high temperature sensitivity. Although its geometry nominally increases the moment of inertia compared to G1, it reached a maximum deformation of 1211.5 mm (1.21 m). This demonstrates that while the rectangular distribution increases stiffness, the presence of constant thicknesses and orthogonal corners remains mechanically inefficient and highly susceptible to the effects of severe thermal expansion. In stark contrast, the G3 configuration achieves the highest structural performance, with a maximum stabilized deformation of only 149 mm (0.149 m). This represents a remarkable 95.7% reduction in maximum displacement compared to the failure of the circular G1 profile. Despite operating under the most severe environmental conditions (100 °C), the contribution of the thermal load in G3 was effectively mitigated, demonstrating that the variable elliptical geometry and longitudinal taper optimally redistributed the gravitational and thermal forces. These results validate the analytical framework presented in Equation 4. For the G1 design, the reduction in E(T) combined with a low I(x) minimizes flexural stiffness, causing the disproportionate increase in theoretical displacement. Conversely, the optimized variable elliptical profile (G3) strategically increases the moment of inertia I(x) in the areas where the bending moment M(x) is maximum. This geometry proactively compensates for the thermal reduction of E(T), maintaining overall bending stiffness and analytically validating the stabilization of deformation at a safe service limit of 149 mm (Table 6). The distribution of these deformation fields is visually compared in Figure 9, where the transition from red (critical displacement) to blue (stability) confirms the efficiency of the optimized elliptical profile.

Von mises stress and safety factor

The multiaxial stress state was evaluated using the Von Mises criterion to capture the interaction between structural bending induced by gravitational loads and the pressure generated by thermal expansion. This criterion is essential for predicting the onset of plastic creep in viscoelastic polymers and thermoplastic composites, such as r-HDPE/GF, under coupled thermomechanical loading conditions [16, 18]. The equivalent stress (σ_{vm}) is calculated as:

Table 6. Maximum total deformation under combined thermomechanical loads

Design ID	Maximum deformation (m)	Maximum deformation (mm)	Location of maximum deformation
G1 – circular	3.4872	3487.2	Free end of the arm (connection to the luminaire)
G2 – rectangular	1.2115	1211.5	Free end of the arm (connection to the luminaire)
G3 – variable elliptical	0.1490	149.0	Free end of the arm (connection to the luminaire)

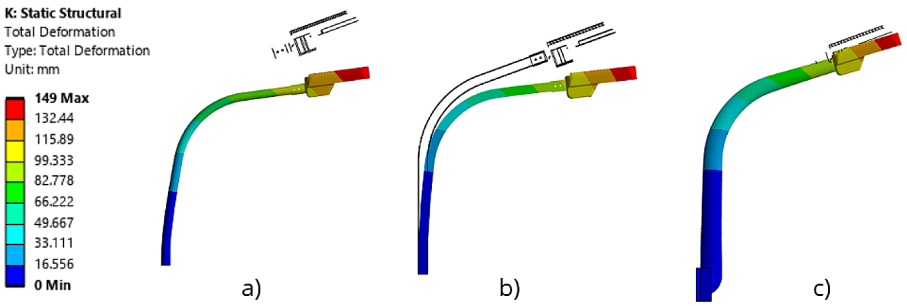


Figure 9. Comparative visualization of the total deformation fields: a) circular profile G1, b) rectangular profile G2 and c) optimized variable elliptical profile G3

$$\sigma_{vm} = \sqrt{\frac{(\sigma_1-\sigma_2)^2 + (\sigma_2-\sigma_3)^2 + (\sigma_3-\sigma_1)^2}{2}} \quad (7)$$

where: σ_1, σ_2, and σ_3 represent the principal stresses. In this study, the equivalent stress results from the superposition of gravitational bending and the internal pressure generated by the thermal gradient ΔT.

Since the recycled HDPE/GF composite is highly temperature-dependent, the structural evaluation uses a localized factor of safety (FS) based on the effective yield strength (σ_y) at the maximum operating temperatures [9, 11]. The FS is defined by the following relationship:

$$SF = \frac{\sigma_y(T)}{\sigma_{vm}} \quad (8)$$

Although the model assigns the same base thermoelastic properties (r-HDPE/GF) to the three simulations, the effective yield strength $\sigma_y(T)$ decreases differentially among the designs because each topology exhibits a distinct heat dissipation pattern (see Table 7). For example, under the same incident irradiance, the rectangular profile (G2) concentrates heat and reaches local temperatures of 97 °C, drastically degrading its yield strength to only 11 MPa, while the circular profile (G1) reaches 94 °C. Stress analysis reveals that both conventional profiles operate under a state of instability and imminent structural failure (FS = 0.26 for G1 and FS = 0.29 for G2). This numerical collapse is a consequence of a severe stress concentration (53.62 MPa and ≈38.01 MPa, respectively) located at the anchorage base, exceeding the residual capacity of the thermally softened material by almost three times. In contrast, the optimized elliptical configuration G3 is the only one that manages to maintain support integrity (FS = 1.57). Despite experiencing higher isothermal heating (=100 °C) that degrades its yield strength to 8.0 MPa, the inertial distribution of the tapered design homogenizes the flow of internal stresses to a maximum of 5.08 MPa. This

Table 7. Comparative analysis of stresses: Von Mises stress versus temperature-dependent elastic limit

Design ID	Maximum von Mises stress (MPa)	Local temperature (°C)	Effective yield strength (MPa)	Stress/yield ratio
G1 – circular	53.62	≈ 94	14	3.83
G2 – rectangular	38.01	≈ 97	11	3.46
G3 – variable elliptical	5.08	100	8	0.64

Table 8. Factores de seguridad (FS) calculados para las secciones críticas del soporte

Design ID	Critical section	Factor de seguridad (FS)	Failure mode trend	Structural assessment
G1 – circular	Unión de base	0.26	Colapso plástico	Falla
G2 – rectangular	Esquina del brazo cerca de la base	0.29	Plástico que se deforma	Falla
G3 – elíptica variable	Zona de transición cónica	1.57	Predominantemente elástico	Seguro

behavior mechanically validates that the variable inertia profile (G3) not only prevents critical stress concentrations at sharp corners or base joints, but also provides the necessary elastic margin to withstand the most severe scenario of prolonged solar radiation exposure.

Structural evaluation and failure tendency

To summarize these effects, Table 8 presents the final structural evaluation. The variable elliptical section (G3) exhibits predominantly elastic behavior with a factor of safety (FS) of 1.57, a performance significantly superior to the critical failure rates found in the circular (0.26) and rectangular (0.29) designs. This marked disparity clearly suggests the need to implement an optimized geometric approach to redistribute thermo-mechanical stresses and prevent plastic creep of the recycled polymer under severe operating loads..

The spatial distribution of these stresses is illustrated in Figure 10, which highlights how the G3 geometry mitigates the stress concentrations that often appear at the sharp vertices of G2.

The maximum Von Mises stresses illustrated in Figure 10 reveal a marked contrast in load-bearing capacity between the profiles, an aspect directly linked to the geometric efficiency of the G3 configuration. Physically, the disproportionate deformation of 3487.2 mm observed in the circular profile (G1) does not represent a stable deformed shape, but rather a complete failure of the structure due to flexural-torsional collapse. This deficiency is explained by the material softening formulation, supported by the kinetics in Equation (5) and the discrete thermoelastic data defined in Table 2, where the yield strength $\sigma_y(T)$ and Young's modulus $E(T)$ decrease drastically at elevated temperatures. As defined in Equation 4, this severe reduction of mechanical parameters, combined with a low and constant moment of inertia $I(x)$ of the G1 profile, critically minimizes flexural stiffness, triggering deformations of collapse proportions.

For the rectangular profile (G2), localized temperatures reach critical levels (97 °C), raising the maximum equivalent stresses to 38.01 MPa and inducing a maximum strain of 1211.5 mm. While the rectangular geometry inherently provides a higher moment of inertia than G1, the high stresses in G2 are strongly concentrated at its orthogonal corners. This leads to localized structural instability and unstable plastic yielding (with a critical safety factor of 0.29), confirming that simply increasing the moment of inertia without proper stress homogenization is insufficient for the r-HDPE/GF composite under these extreme environmental conditions.

In contrast, the variable elliptical profile (G3) comprehensively resolves both failure modes. Its design features longitudinal taper that

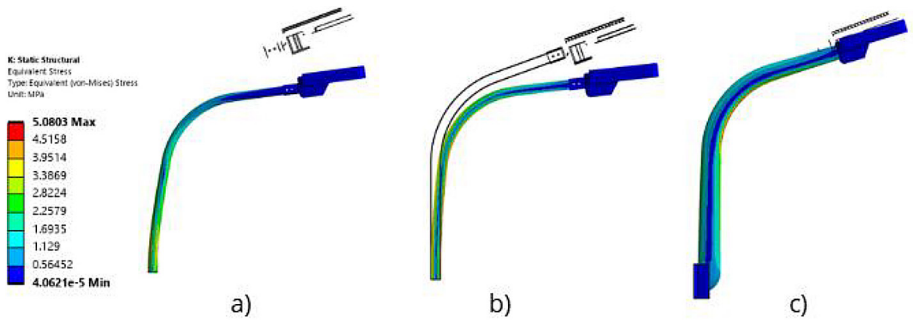


Figure 10. Von Mises stress distribution and critical regions for: a) rectangular configurations G2 and b) variable elliptical configurations G3

structurally increases the moment of inertia $I(x)$ precisely in the areas where the thermal decay of Young's modulus $E(T)$ and the increase in bending moment $M(x)$ are most critical. Additionally, this topology shifts the center of mass toward the anchorage base, reducing the lever arm of gravity and, consequently, the total applied moment. By eliminating sharp vertices, the G3 profile achieves a uniform stress gradient, registering a maximum stabilized stress of only 5.08 MPa. This drastic stress reduction confirms that the G3 configuration provides a robust mechanical foundation, preserves overall bending stiffness, and effectively mitigates the load-bearing capacity loss induced by thermal softening of the composite material.

Multi-scale service life analysis

To bridge the gap between short-term thermal kinetics and long-term urban operational requirements, a multi-scale simulation was performed. This approach moves from transient daily cycles to a ten-year service life projection.

Transient thermal response and incipient damage

While the isothermal degradation curves in the Thermal Gradients and Degradation Indicators section assume constant maximum exposure, actual conditions include periods of nighttime cooling. Figure 11 illustrates the first 168 hours of service under cyclic thermal loads (day: 100 °C / night: 25 °C). Analytically, the oscillation of the surface temperature T(t) over time is modeled by a periodic distribution function based on the insolation curve:

$$T(t) = T_{min} + (T_{max} - T_{min}) \cdot f_{suvizado}(t) \quad (9)$$

where: T_{min} = 25 °C represents the nighttime base temperature and T_{max} = 100 °C corresponds to the maximum daytime thermal peak recorded in profile G3, performing the calculations in the worst case scenario.

Complementarily, the retained structural integrity $R(t)$ is governed by the accelerated aging kinetics:

$$R(t) = 1.0 - k\left(\frac{t}{t_{total}}\right)^n \quad (10)$$

The simulation reveals a cyclic ratchet effect, where the material undergoes repeated thermomechanical expansions and contractions. While structural integrity remains above 99.5% during this first week, the infinitesimal microstructural damage accumulated during each thermal oscillation peak confirms that degradation begins from the first day of service. This daily rate serves as a fundamental input for the long-term cumulative model.

Cumulative projection over 10 years

By integrating the daily damage rates into a nonlinear sigmoidal decay function, a ten-year projection was achieved, modeled by the following analytical relationship:

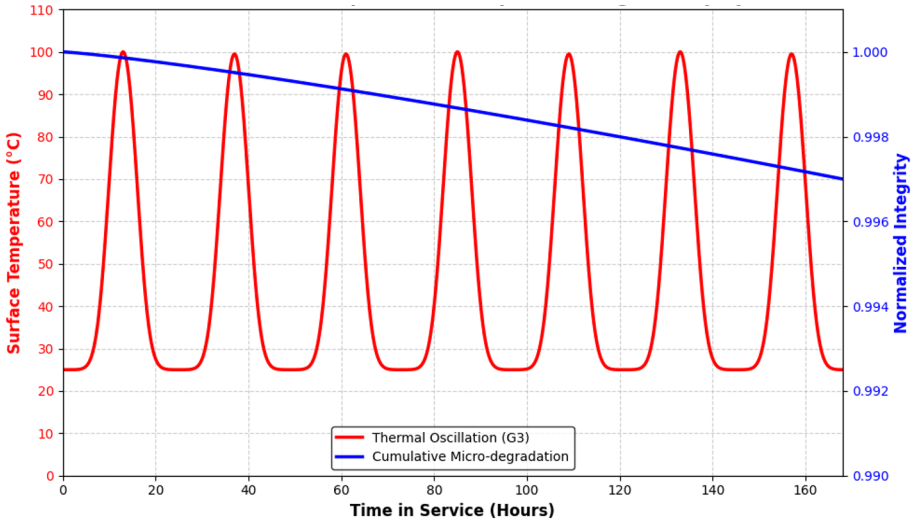


Figure 11. Transient thermal response and incipient damage accumulation of the r-HDPE/GF composite during a 168-hour operating cycle (day: 100 °C / night: 20 °C)

$$R(t) = \frac{1.0}{1.0+\exp\left(k\cdot(t-t_f)\right)} \quad (11)$$

where: t_f is the critical failure time (years) and k is the degradation sensitivity coefficient.

For profile G2 (rectangular), a rate constant k_{G2} = 1.19 was determined, while for design G3 (variable elliptical) a reduced value of k_{G3} = 0.66 was obtained, reflecting its greater structural stability. This projection, illustrated in Figure 12, represents the maximum functional limit of the infrastructure under variable environmental conditions.

The evidence supporting G3's superior performance lies in the optimization of its second moment of inertia, I(x). Although the material is identical across all designs, G3's variable elliptical geometry provides a higher average moment of inertia. As demonstrated in the stress maps in Figure 10, G3 achieves a lower average stress state and a more uniform distribution; this, combined with a geometry that minimizes thermal stresses, results in significantly greater flexural stiffness.

Consequently, as illustrated in Figure 12, this structural efficiency directly determines the service life. While the rectangular profile (G2) reaches the critical brittleness threshold (50%) at approximately 5.8 years, the optimized thermal management and reduced stress state of the G3 design extend this threshold to 10.4 years. This 4.6-year service life extension (a 79% increase) validates the proposed geometric configuration as a strategic requirement for the viable implementation of recycled composite polymers in urban infrastructure.

Considerations on mitigating progressive deformation and environmental degradation

Regarding long-term structural stability, the optimized variable inertia of the G3 profile serves as a proactive engineering strategy to mitigate creep deformation under sustained thermal loading. Experimental studies [5, 7] have shown that when stress levels applied to HDPE composites are kept below 60% of their ultimate strength, the material remains within the stable (secondary) creep phase, effectively preventing severe necking instability or tertiary creep. In this study, the G3 configuration redistributes thermomechanical loads to maintain a maximum Von Mises stress of 5.08 MPa versus a thermally degraded creep strength of 8.0 MPa at 100 °C. Consequently, the design operates at a stress ratio of 0.64 (64%), mathematically ensuring that it remains within the projected safety margins and preventing accelerated creep. Furthermore, based on the power-law dependence of creep failure analyzed in mathematical models [5], the massive reduction of localized stress at peak temperatures significantly extends the time to failure, validating the projected service life of 10.4 years.

Regarding environmental factors, this research prioritizes thermal degradation over UV-induced degradation as the primary cause of structural softening. While UV radiation

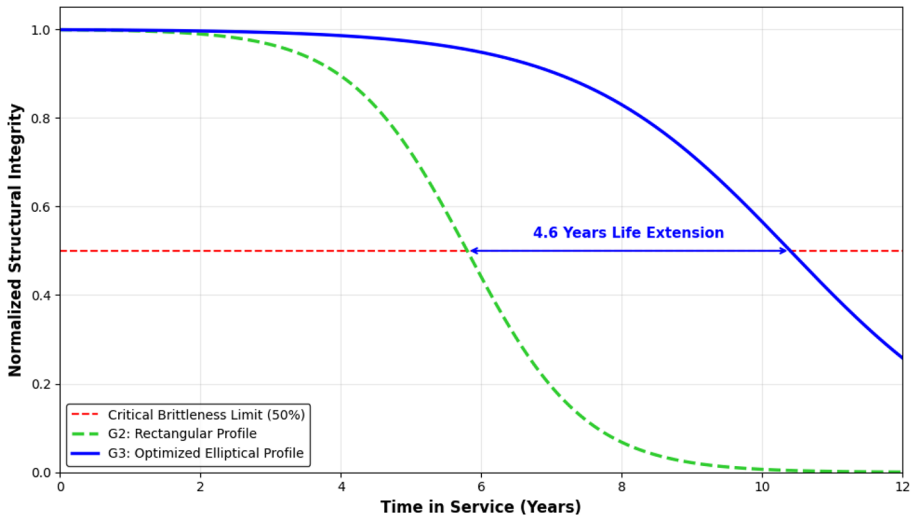


Figure 12. Projection of cumulative structural degradation over ten years comparing profiles G2 and G3 in relation to the critical fragility limit (50%)

causes surface microcracks, initial exposure often induces molecular crosslinking, which can temporarily increase the Young's modulus and creep resistance of the polymer [6]. In contrast, the thermal softening induced by solar radiation, modeled in this study, represents a volumetric phenomenon that causes an immediate loss of flexural stiffness due to the material's low thermal conductivity, as documented in previous studies on thermo-oxidative degradation [8, 9]. Therefore, by focusing on thermal degradation, this model adopts a conservative "worst-case" scenario for load-bearing capacity, as it considers the overall softening of the structure, omitting the temporary surface hardening effects of UV-induced crosslinking. To address the inherent variability in the thermomechanical properties of post-consumer recycled polymers (r-HDPE/GF), the sensitivity of structural performance to a theoretical 10% penalty in Young's Modulus and Base Yield Strength was evaluated. Under this degraded scenario, the maximum deformation of the G3 profile experienced a marginal increase, stabilizing below 165 mm, while the factor of safety (FS) remained above the critical threshold of 1.2. This low parametric sensitivity confirms that the geometric inertia of the variable elliptical configuration effectively absorbs material uncertainties, supporting structural viability even with suboptimal recycling batches.

CONCLUSIONS

This study indicates the structural and temporal viability of the r-HDPE/GF composite for urban infrastructure through strategic geometric redesign. By addressing the inherent thermal sensitivity of the polymer matrix, the research demonstrates that the transition from conventional geometries to optimized cross-sections is a fundamental requirement for the reliable implementation of recycled composite materials in load-bearing applications.

The results indicate that structural integrity is primarily governed by the moment of inertia of the cross-section and its capacity to redistribute thermomechanical stresses. Specifically, the variable elliptical configuration (G3) achieved a 95.7% reduction in maximum displacement compared to the reference circular profile (G1), which exhibited severe deformation of 3487.2 mm, exceeding stability limits. This improvement is attributed to the optimized material distribution along the longitudinal axis, maintaining the maximum deformation of the G3 configuration within a functional and safe limit of 149.0 mm. Furthermore, multiaxial stress analysis confirmed that geometric optimization effectively mitigates the "thermal softening" effect characteristic of the r-HDPE/GF composite. The following findings highlight the mechanical robustness of the proposed design:

- Structural integrity: The G3 profile maintains a FS of 1.57, operating within the elastic range under extreme conditions of 100 °C. In contrast, the circular (G1) and rectangular (G2) designs reached structural collapse states with critical factors of safety of 0.26 and 0.29, respectively.
- Parametric robustness: The G3 design demonstrates significant stability against variations in material properties and mesh parameters, overcoming the inherent variability of recycled raw materials. This supports the reliable maintenance of structural performance even in the face of the physical inconsistencies typical of post-consumer r-HDPE/GF composites.
- Parametric robustness: The G3 design demonstrates significant stability against variations in material properties and mesh parameters, overcoming the inherent variability of recycled raw materials. This supports the claim that structural performance remains reliable even in the face of the physical inconsistencies typical of post-consumer r-HDPE/GF composites.
- Lifespan projection: The multiscale degradation model established a significant milestone in terms of durability, extending the infrastructure's lifespan to 10.4 years, compared to 5.8 years for the rectangular profile (G2). This represents a 79% increase in longevity, directly contributing to circular economy goals by promoting a decade of operational reliability.

This research provides a robust technical framework for replacing conventional materials with sustainable alternatives in street furniture. This structural performance is consistent with the serviceability limit state principles established in international standards for lighting supports, such as AASHTO LTS-6 and EN 40-3-3. Although thermoplastic polymers exhibit greater inherent bending than conventional steel, the stabilization of the maximum deformation of the G3 profile at 149 mm (approximately L/30 of the effective arm length) ensures system integrity without

compromising urban clearances or inducing low-cycle fatigue, suggesting its safe implementation. This methodology consolidates polymer upcycling and establishes an extrapolable approach for the structural optimization of green urban infrastructure

Ackonwledgments

We thank the National University of San Agustín of Arequipa for their support and knowledge.

REFERENCES

1. van Hees M, Oskam I, Bocken N. Motives, drivers and barriers to urban upcycling: Insights from furniture upcycling in the Netherlands. J Clean Prod. 2025;486:144485. https://doi.org/10.1016/j.jclepro.2024.144485
2. Ogwu MC, Kosoe EA. Innovative approaches to recycling, upcycling, and material repurposing for sustainable waste management. CleanMat. 2025;2:242–261. https://doi.org/10.1002/clem.70013
3. Khairul Anuar SZ, et al. Recent advances in recycling and upcycling of hazardous plastic waste: A review. J Environ Manage. 2025;380:124867. https://doi.org/10.1016/j.jenvman.2025.124867
4. Skandali C, et al. Reviewing the parameters that affect sustainability and energy efficient concepts in road and urban lighting design. J Clean Prod. 2025;490:144607. https://doi.org/10.1016/j.jclepro.2024.144607
5. Mao Q, Su B, Ma R, Li Z. Investigation of tensile creep behavior for high-density polyethylene (HDPE) via experiments and a mathematical model. Materials. 2021;14:6188. https://doi.org/10.3390/ma14206188
6. Becerra AFC, d'Almeida JRM. UV effects on the tensile and creep behaviour of HDPE. Polymers and Polymer Composites. 2017;25:327–332. https://doi.org/10.1177/096739111702500502
7. Amjadi M, Fatemi A. Creep behavior and modeling of high-density polyethylene (HDPE). Polym Test. 2021;94:107031. https://doi.org/10.1016/j.polymertesting.2020.107031
8. Albin Zaid ZAA, Otaru AJ. Low-heating-rate thermal degradation of date seed powder and HDPE plastic: Machine learning CDNN, MLRM, and thermokinetic analysis. Polymers (Basel). 2025;17:740. https://doi.org/10.3390/polym17060740
9. Cuadri AA, Martín-Alfonso JE. The effect of thermal and thermo-oxidative degradation conditions on rheological, chemical and thermal properties of HDPE. Polym Degrad Stab. 2017;141:11–18. https://doi.org/10.1016/j.polymdegradstab.2017.05.005
10. Zhao J, et al. Solar radiation transfer and performance analysis of an optimum photovoltaic/thermal system. Energy Convers Manag. 2011;52:1343–1353. https://doi.org/10.1016/j.enconman.2010.09.032
11. Spychała MJ, et al. Structural and mechanical properties of recycled HDPE with milled GFRP as a filler. Materials. 2024;17:5875. https://doi.org/10.3390/ma17235875
12. Huang R, et al. High density polyethylene composites reinforced with hybrid inorganic fillers: Morphology, mechanical and thermal expansion performance. Materials. 2013;6:4122-4138. https://doi.org/10.3390/ma6094122
13. Qureshi J. A review of recycling methods for fibre reinforced polymer composites. Sustainability. 2022;14. https://doi.org/10.3390/su142416855
14. Obaid N, Kortschot MT, Sain M. Modeling and predicting the stress relaxation of composites with short and randomly oriented fibers. Materials. 2017;10(10):1207. https://doi.org/10.3390/ma10111207
15. Castricum BA, Fagerström M, Ekh M, Larsson F, Mirkhalaf SM. A computationally efficient coupled multi-scale model for short fiber reinforced composites. Composites Part A: Applied Science and Manufacturing. 2022;163:107233. https://doi.org/10.1016/j.compositesa.2022.107233
16. Smetannikov O, Sakhabutdinova L, Ilyinykh G. ANSYS simulation of the thermomechanical behavior of a large-sized composite mandrel with consideration of viscoelasticity. Aerospace. 2022;9:117. https://doi.org/10.3390/aerospace9030117
17. Smyczyński MJ, Paczos P, Pruszyński J, Kasprzak J. Stability of selected open and closed thin-walled beams: numerical analysis. Advances in Science and Technology Research Journal. 2026;20:318–339. https://doi.org/10.12913/22998624/211003
18. Cho JR. Large deflection geometrically nonlinear bending of porous nanocomposite cylindrical panels on elastic foundation. Symmetry. 2024;16:224. https://doi.org/10.3390/sym16020224
19. AASHTO. (2013). Standard Specifications for Structural Supports for Highway Signs, Luminaires, and Traffic Signals (6th ed.). American Association of State Highway and Transportation Officials.
20. CEN. (2003). EN 40-3-3: Lighting columns - Part 3-3: Design and verification - Verification by calculation. European Committee for Standardization.